Supplemental Materials to Investigating the association between late spring Gulf of Mexico sea surface temperatures and US Gulf Coast precipitation extremes with focus on Hurricane Harvey

Brook T. Russell* Mark D. Risser † Richard L. Smith ‡

Ken Kunkel § ¶

July 23, 2019

1 Simulation Studies

In order to assess the viability of our proposed method, we conduct two simulation studies. The results are presented in this Section.

*Clemson University Department of Mathematical Sciences, Clemson, SC 29634 (email: brookr@clemson.edu, office: 864-656-4571, fax: 864-656-5230)

†Lawrence Berkeley National Lab, Berkeley, CA 94720

‡University of North Carolina–Chapel Hill Department of Statistics and Operations Research, Chapel Hill, NC 27599

§North Carolina State University Department of Marine, Earth, and Atmospheric Sciences, Raleigh, NC 27695

¶Cooperative Institute for Climate and Satellites–NC, Asheville, NC 28801

1.1 Simulation Study 1

For $\mathcal{D} \subset \mathbb{R}^2$, we consider D, a finite set of equally spaced grid points in $\mathcal{D}$. For all $\boldsymbol{s} \in D$, we randomly generate true location, scale, and shape fields ($\mu(\boldsymbol{s})$, $\sigma(\boldsymbol{s})$, and $\xi(\boldsymbol{s})$ respectively) using a Gaussian process with Matérn covariance structure. Based on these fields we also obtain $RL(\boldsymbol{s})$, the true 100 year return level at $\boldsymbol{s}$. For the nth simulation ($n = 1, \ldots, N$) we simulate $Z_a(\boldsymbol{s})$ ($a = 1, \ldots, A$), independent realizations from a max-stable process with unit Fréchet margins for l randomly selected $\boldsymbol{s} \in D$. For a set of randomly selected locations $L \subset D$, we transform to $GEV(\mu(\boldsymbol{s}), \sigma(\boldsymbol{s}), \xi(\boldsymbol{s}))$ margins for each $\boldsymbol{s} \in L$ using the probability integral transformation

$$Y_a(\boldsymbol{s}) = G^{-1}_{\mu(\boldsymbol{s}),\sigma(\boldsymbol{s}),\xi(\boldsymbol{s})}[F(Z_a(\boldsymbol{s}))],$$

where F is the unit Fréchet distribution function and $G_{\mu(\boldsymbol{s}),\sigma(\boldsymbol{s}),\xi(\boldsymbol{s})}$ is the distribution function for a random variable that has the $GEV(\mu(\boldsymbol{s}), \sigma(\boldsymbol{s}), \xi(\boldsymbol{s}))$ distribution. For all $\boldsymbol{s} \in L$, we obtain the series of maxima $(Y_1(\boldsymbol{s}), \ldots, Y_A(\boldsymbol{s}))$ and use the procedure outlined in our manuscript to estimate $\mu(\boldsymbol{s})$, $\sigma(\boldsymbol{s})$, $\xi(\boldsymbol{s})$, and $RL(\boldsymbol{s})$ for all $\boldsymbol{s} \in D$ using $\lambda \in \Lambda = \{\lambda_1, \ldots, \lambda_r\}$ for $r < \infty$. For each n and each choice of λ, we calculate

$$SSE^{(n)}_\lambda = \sum_{\boldsymbol{s} \in D} [RL(\boldsymbol{s}) - \widehat{RL}^{(n)}_\lambda(\boldsymbol{s})]^2$$

where $RL(\boldsymbol{s})$ is the true 100 year return level at $\boldsymbol{s}$, and $\widehat{RL}^{(n)}_\lambda(\boldsymbol{s})$ is the estimated 100 year return level for the nth simulated data set based on λ. For each $\lambda \in \Lambda$, we calculate the 0.25 quantile, the 0.5 quantile, the 0.75 quantile, and the mean of $SSE^{(1)}_\lambda, \ldots, SSE^{(N)}_\lambda$.

In our simulation study, we choose $A = 100$, $l = 50$, $N = 500$[1], D to be a

[1]We note that there were convergence issues on three of the 500 simulations, and these three

50×50 grid of points on $[0, 10]^2$, and simulate from the Schlather max-stable process with powered exponential covariance model Schlather (2002). We take $\Lambda = \{0, 0.5, 1.0, 1.5, 2.0, \infty\}$, where $\lambda = 0$ corresponds to the sparse banded covariance matrix and $\lambda = \infty$ corresponds to using the unadjusted bootstrap covariance matrix. The randomly generated location, scale, and shape fields are given in Figure 1, along with the resulting 100 year return level. The results of this simulation study are summarized in Table 1. These results suggest that it may be possible to improve return level estimates by choosing a sensible λ.

Table 1: For each procedure in Simulation Study 1, we present the 0.25 quantile, the 0.5 quantile, the 0.75 quantile, and the mean of $SSE_\lambda^{(1)}, \ldots, SSE_\lambda^{(N)}$ for all $\lambda \in \Lambda$.

	Banded	$\lambda = 0.5$	$\lambda = 1.0$	$\lambda = 1.5$	$\lambda = 2.0$	BS Cov Mat
25%	23937.67	21994.63	22041.15	22043.21	23307.09	55728.17
50%	37537.99	37106.37	36324.92	36298.84	37954.90	167390.83
75%	67169.95	64154.69	64062.09	65644.18	72238.34	440925.37
Mean	58223.92	58035.93	55097.87	58026.86	64704.03	1144228.14

1.2 Simulation Study 2

For $\mathcal{D} \subset \mathbb{R}^2$, we consider D, a finite set of equally spaced grid points in $\mathcal{D}$. For all $\boldsymbol{s} \in D$, we randomly generate true fields $\theta_1(\boldsymbol{s}), \ldots, \theta_5(\boldsymbol{s})$. We use a Gaussian process with Matérn covariance structure to generate $\theta_1(\boldsymbol{s}), \theta_3(\boldsymbol{s}), \theta_5(\boldsymbol{s})$ and $\theta_2(\boldsymbol{s}), \theta_4(\boldsymbol{s})$ are linear trend surfaces. These five fields are used to create the location, scale, and shape values at $\boldsymbol{s}$ via

$$\begin{aligned} \mu_t(\boldsymbol{s}) &= \theta_1(\boldsymbol{s}) + t\,\theta_2(\boldsymbol{s}) \\ \log \sigma_t(\boldsymbol{s}) &= \theta_3(\boldsymbol{s}) + t\,\theta_4(\boldsymbol{s}) \\ \xi(\boldsymbol{s}) &= \theta_5(\boldsymbol{s}), \end{aligned}$$

were omitted.

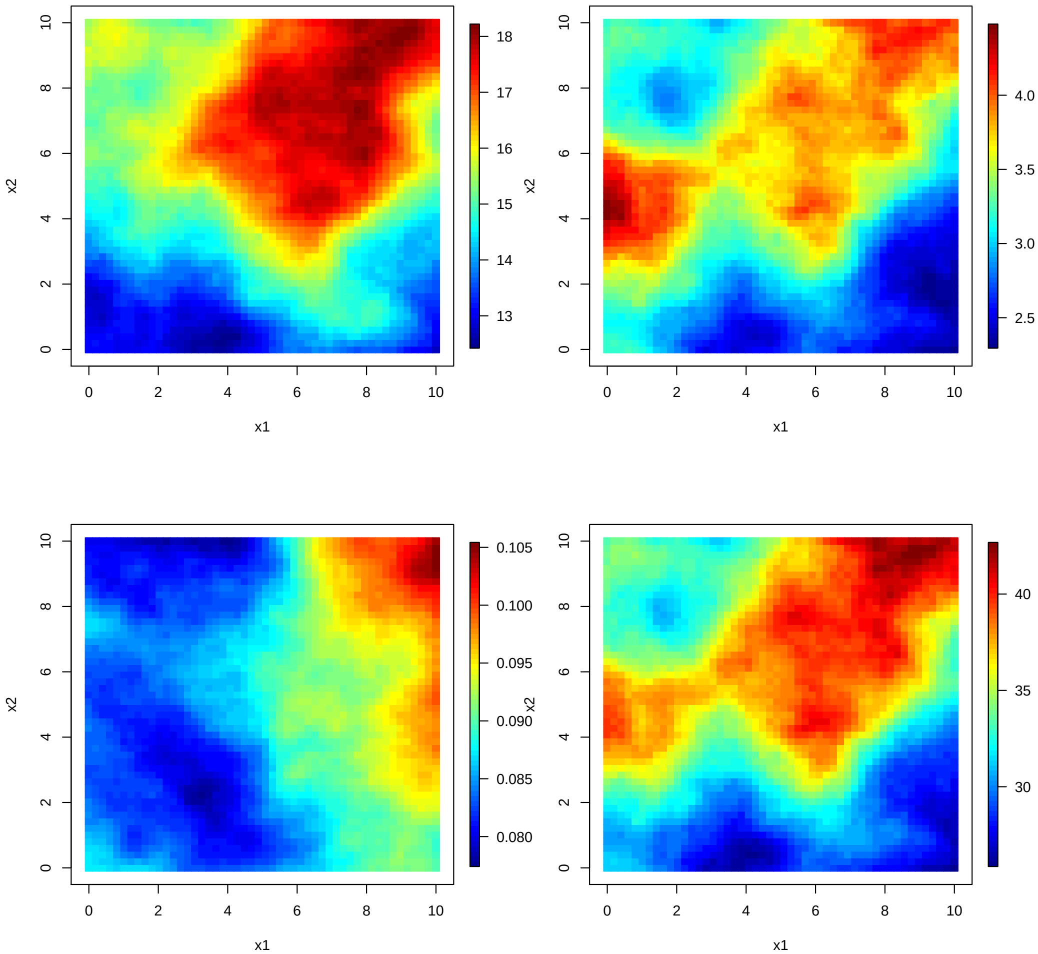

Figure 1: For Simulation Study 1, the top left panel gives the true location field, the top right panel gives the true scale field, the bottom left panel gives the true shape field, and the bottom right panel gives the true 100 year return level values.

where $t = 1, \ldots, T$. Based on these fields we also obtain $RL(\boldsymbol{s})$, the true 100 year return level at $\boldsymbol{s}$ for $t = t'$. For the nth simulation ($n = 1, \ldots, N$) we simulate $Z_a(\boldsymbol{s})$ ($a = 1, \ldots, A$), independent realizations from a max-stable process with unit Fréchet margins for l randomly selected $\boldsymbol{s} \in D$. For a set of randomly selected locations $L \subset D$, we transform to $GEV(\mu(\boldsymbol{s}), \sigma(\boldsymbol{s}), \xi(\boldsymbol{s}))$ margins for each $\boldsymbol{s} \in L$ using the probability integral transformation

$$Y_a(\boldsymbol{s}) = G^{-1}_{\mu(\boldsymbol{s}),\sigma(\boldsymbol{s}),\xi(\boldsymbol{s})}[F(Z_a(\boldsymbol{s}))],$$

where F is the unit Fréchet distribution function and $G_{\mu(\boldsymbol{s}),\sigma(\boldsymbol{s}),\xi(\boldsymbol{s})}$ is the distribution function for a random variable that has the $GEV(\mu(\boldsymbol{s}), \sigma(\boldsymbol{s}), \xi(\boldsymbol{s}))$ distribution. For all $\boldsymbol{s} \in L$, we obtain the series of maxima $(Y_1(\boldsymbol{s}), \ldots, Y_A(\boldsymbol{s}))$ and use the procedure outlined in our manuscript to estimate $\theta_1(\boldsymbol{s}), \ldots, \theta_5(\boldsymbol{s})$ for all $\boldsymbol{s} \in D$ using $\lambda = \lambda'$. For each n and each field, we use the method outlined in our manuscript to obtain estimated fields $\hat{\theta}_1^{(n)}(\boldsymbol{s}), \ldots, \hat{\theta}_5^{(n)}(\boldsymbol{s})$.

In our simulation study, we choose $A = 100$, $l = 50$, $T = 50$ $\lambda' = 0.5$, $N = 500$, D to be a 50×50 grid of points on $[0, 10]^2$, and simulate from the Schlather max-stable process with powered exponential covariance model Schlather (2002). The randomly generated fields are given in the left panels of Figure 2. For all $\boldsymbol{s} \in D$, the pointwise median estimated surfaces are given in Figure 2. We note that the pointwise median surfaces seem to estimate the true surfaces reasonably well, with the exception of the shape parameter, which seems to be underestimated throughout D.

2 Figures

In order to reduce the length of the manuscript, several figures have been moved to this Section.

References

Schlather, M. (2002). Models for stationary max-stable random fields. *Extremes*, 5(1):33–44.

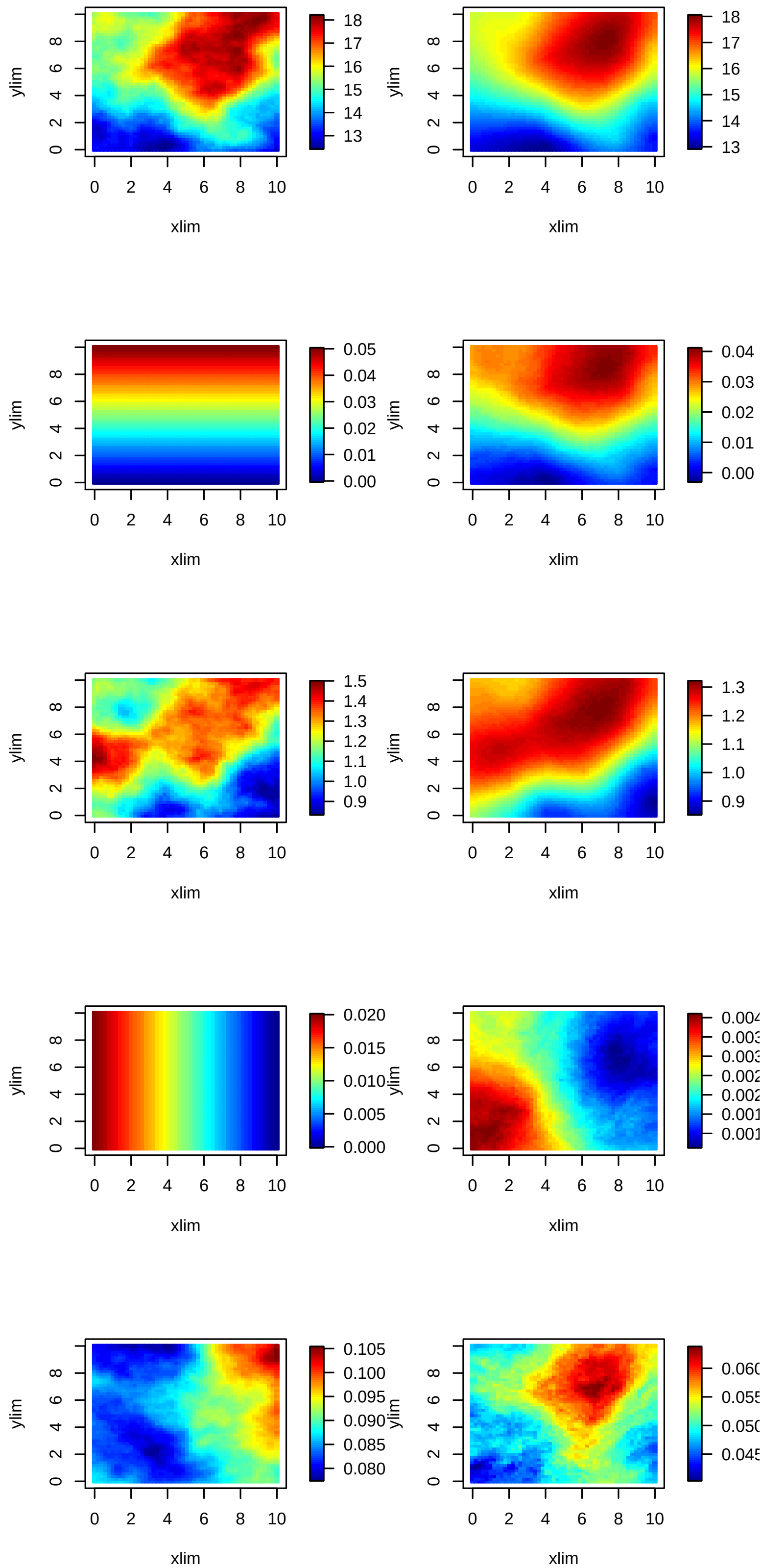

Figure 2: In the left panels, we plot the true surfaces θ_1 to θ_5 (top to bottom) used in Simulation Study 2. In the right panels, we plot the corresponding pointwise median estimated surfaces.

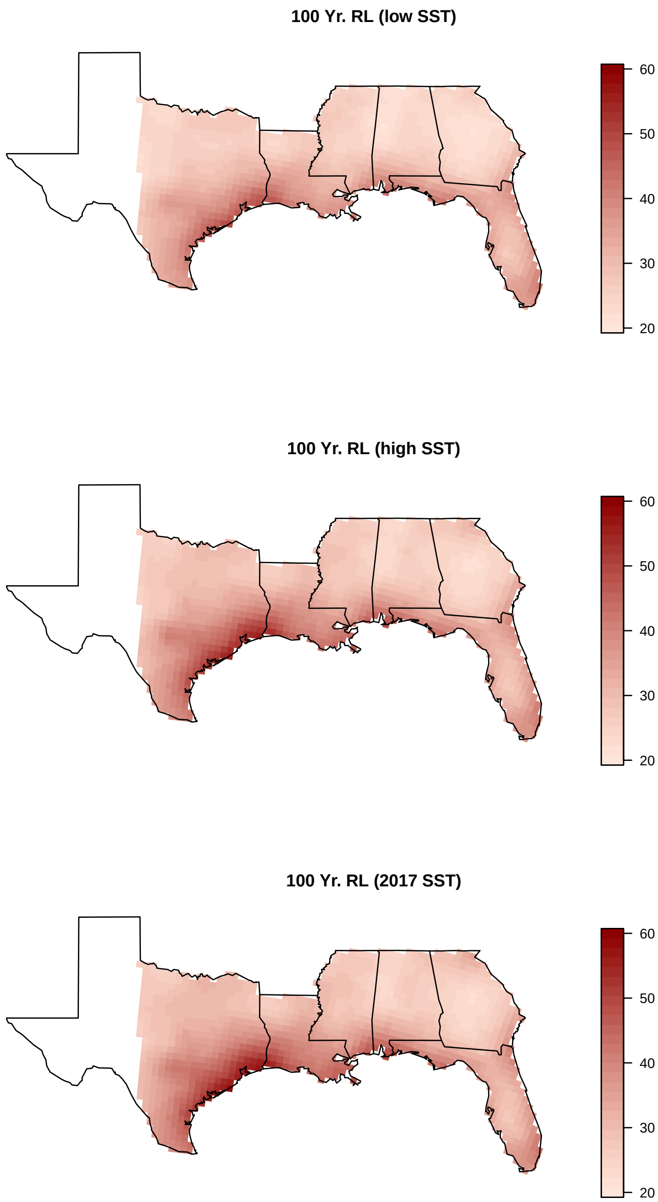

Figure 3: We plot the estimated 100-year return levels (in cm) for low SST (top), high SST (middle), and 2017 SST (bottom).

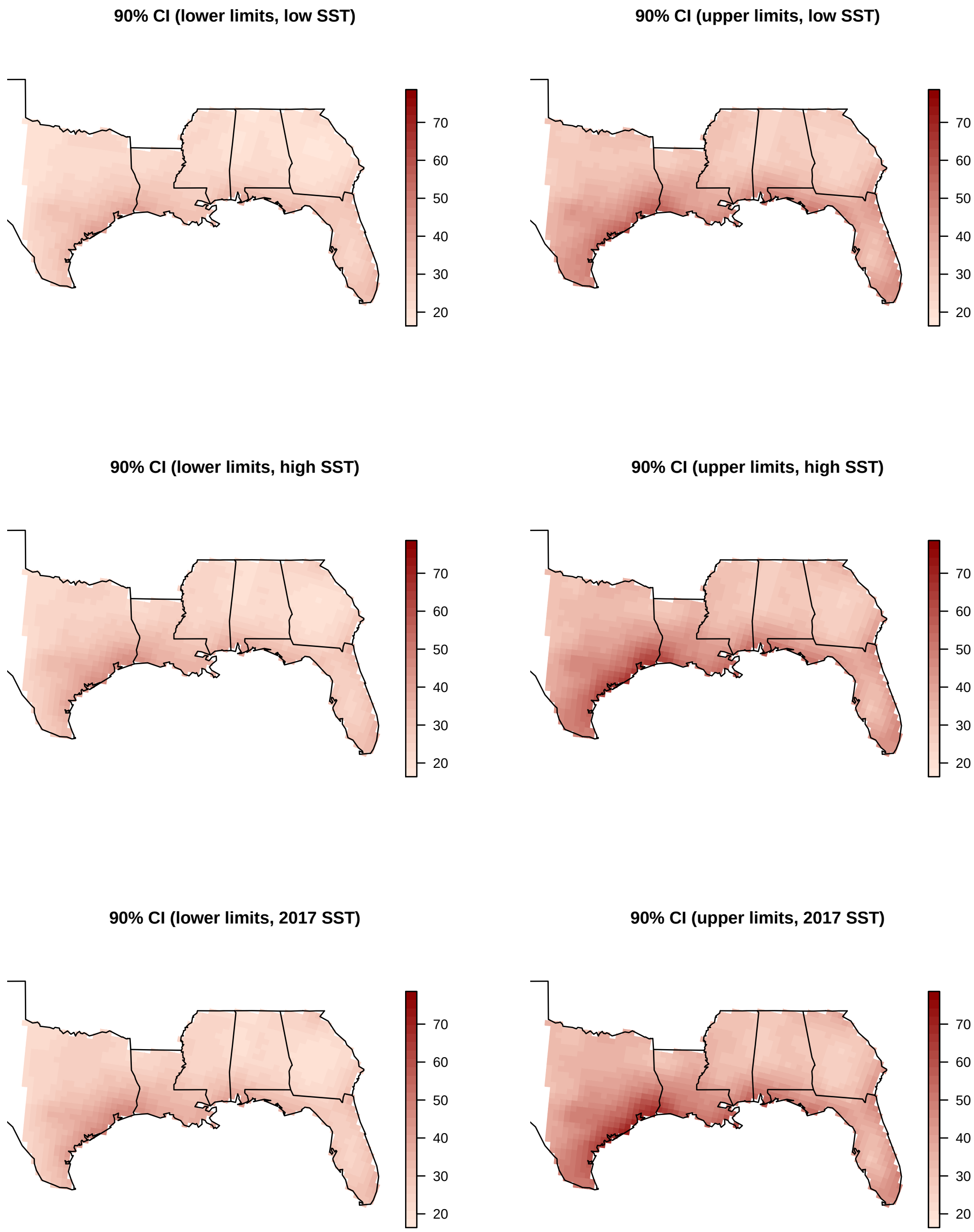

Figure 4: We plot the lower endpoints (left column) and upper endpoints (right column) of the pointwise 90% confidence intervals for the 100-year return levels (in cm). The top row corresponds to low SST, the middle row corresponds to high SST, and the bottom row corresponds to 2017 SST. Confidence intervals are generated via the simulation based method.

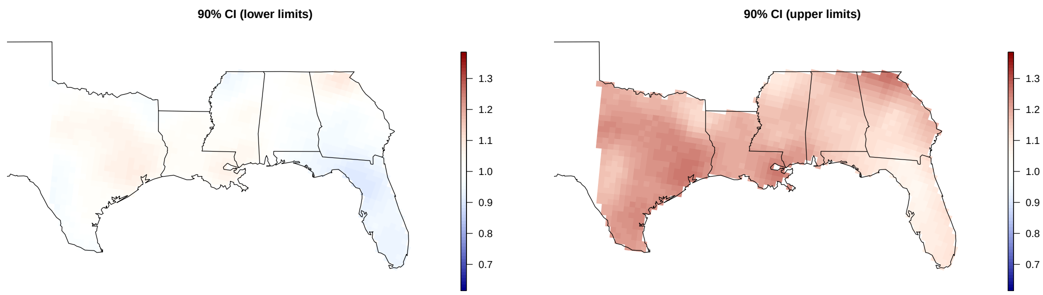

Figure 5: We plot the upper (L) and upper (R) endpoints for the pointwise 90% confidence intervals for the ratio of 100-year return levels (high versus low). Confidence intervals are generated via the simulation based method.

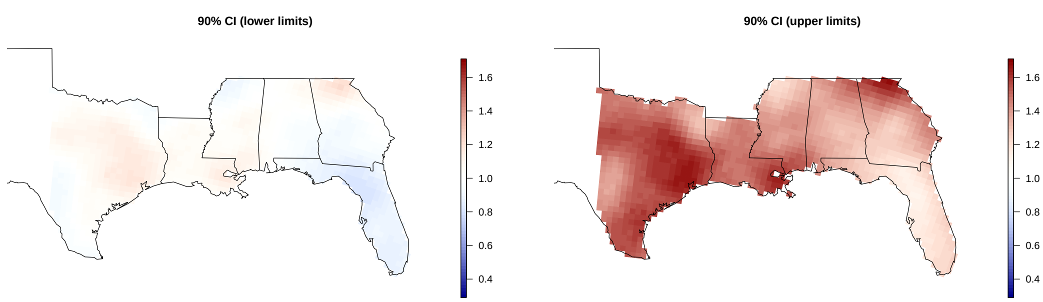

Figure 6: We plot the upper (L) and upper (R) endpoints for the pointwise 90% confidence intervals for the ratio of 100-year return levels (2017 versus low). Confidence intervals are generated via the simulation based method.

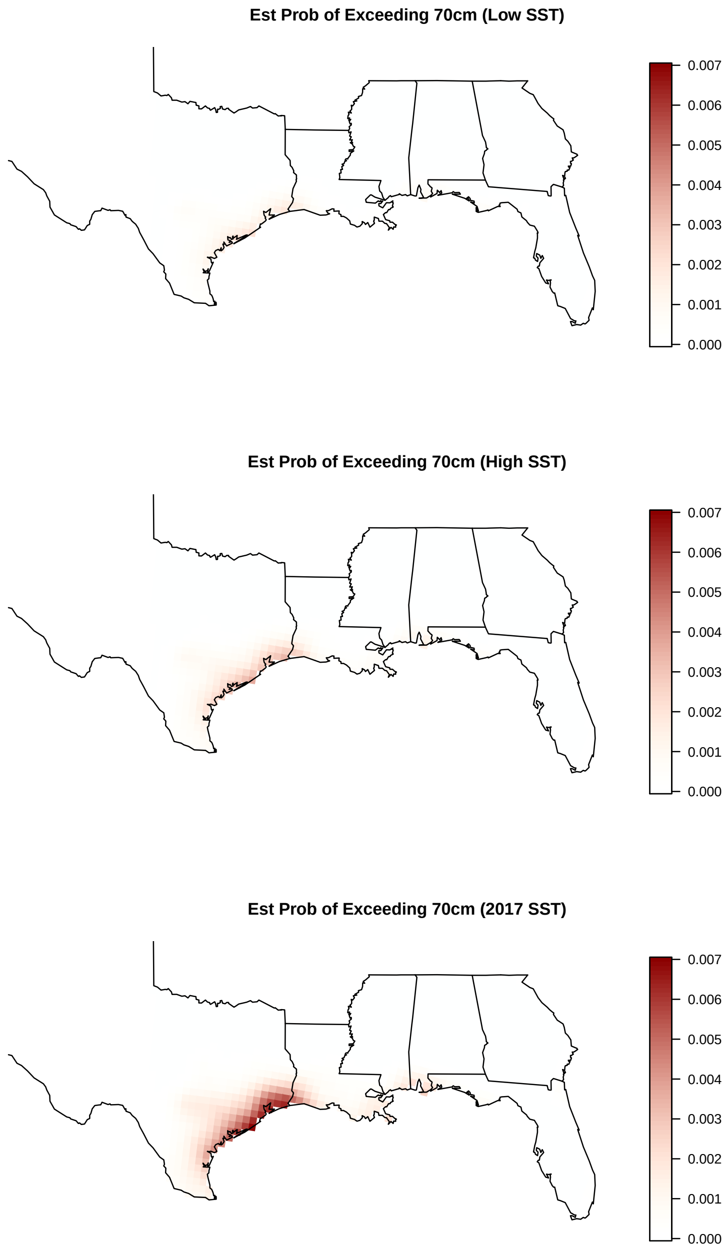

Figure 7: Based on output from our fitted model, we plot the estimated probability of observing a seven-day hurricane season precipitation total in excess of 70 cm for low SST (top panel), high SST (middle panel), and 2017 SST (bottom panel).

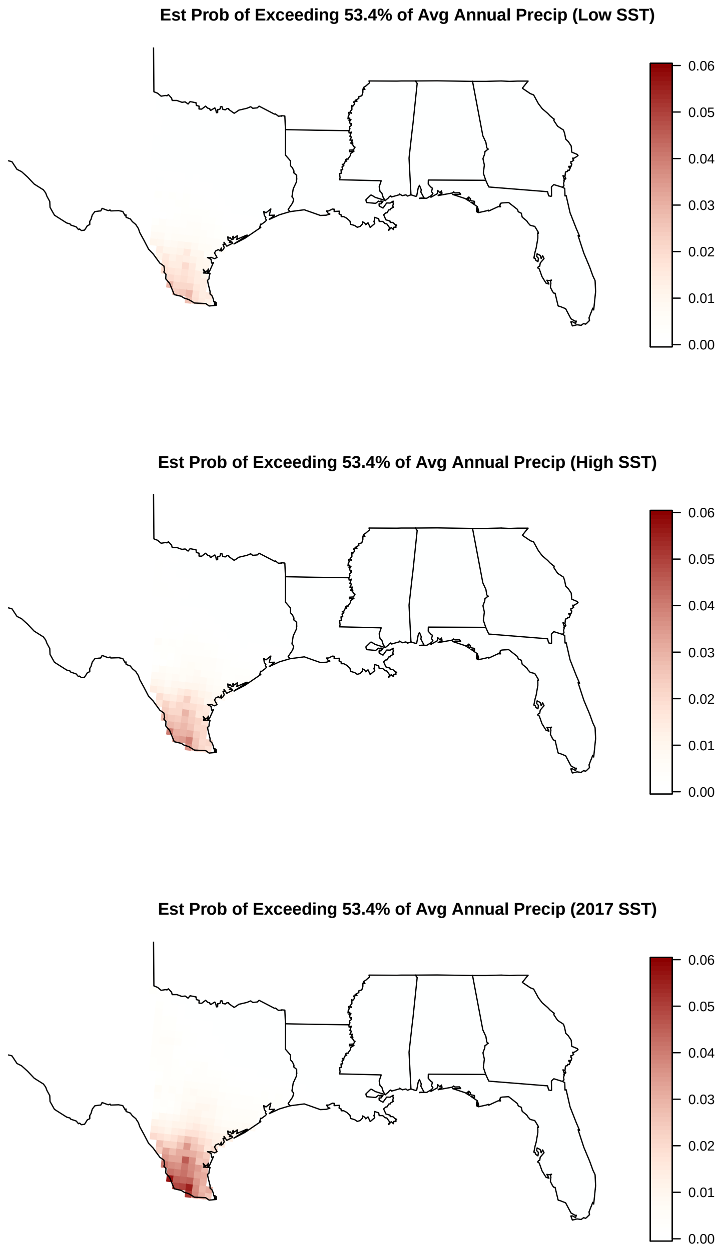

Figure 8: Based on output from our fitted model, we plot the estimated probability of observing a seven-day hurricane season precipitation total in excess of 53.4% of each location's annual average precipitation (corresponding to 70 cm in Houston) for low SST (top panel), high SST (middle panel), and 2017 SST (bottom panel).